H & T PUBLISHER

Volume 2021, 1-11 | Article ID : IJMSI-2106282112360

International Journal of Material Science Innovations

Journal homepage: http://htpub.org/ International-Journal-Of-Material-Science-Innovations/

ISSN: 2289-4063

Steady State Photo-carrier Grating (SSPG) for minority carrier diffusion length analysis in silicon thin films

Deepika Chaudhary[a,b,c], Mansi Sharma,[a,b] and Sushil Kumar[a,b,*]

[a] *Advanced Materials & Device Metrology Division, CSIR – National Physical Laboratory, Dr. K.S. Krishnan Marg, New Delhi, India 110012*

[b] *Academy of Scientific and Innovative Research (AcSIR), CSIR-NPL Campus, New Delhi, Dr. K.S. Krishnan Marg, New Delhi, India 110012*

[c] *Gautam Buddha University, Greater Noida, Uttar Pradesh, India 201312*

Article

Article history:
Received: 10th June 2021
Received in revised form: 28th June 2021
Accepted: 28th June 2021

Keywords:
SSPG; intensity of the probe laser beam; a-Si:H/ nc-Si:H/μc-Si:H thin film; ambipolar diffusion length

Abstract

The ambipolar diffusion length (Ld) is estimation of the diffusion length of less mobile charge carriers (presumably holes) which determines the performance of solar cells. The Steady State Photo-carrier Grating (SSPG) technique measures ambipolar diffusion length in mobility photoconductive semiconductor films. This technique also provide access to the minority carrier transport properties as diffusion length is proportional to the product of mobility (μ) and lifetime (τ) of charge carriers. SSPG measures the interference pattern created by the superposition of two coherent laser beams (L1 and L2). The brief description of this method was presented. Furthermore, the efforts were made to understand the larger attenuated intensity of the laser beam (L2) for the interference fringes can lead to large errors in the measured diffusion length. Moreover, estimation of minority carrier transport in hydrogenated amorphous silicon (a-Si:H) and micro/nano-crystalline thin film (nc-Si:H/μc-Si:H), deposited by PECVD process were carried out. The ambipolar diffusion length in a-Si:H films found to vary from 0.23 ─ 0.11 μm for different photo-gain (� 6 x 104 to 8 x 102) and in nc-Si:H/μc-Si:H vary from 0.190 ─ 0.080 μm for different crystalline fraction (43 % - 22 %). From these results, Ld were observed to be maximum for the film having high photo-gain in a-Si:H and high crystalline fraction in nc-Si:H/μc-Si:H..

1. Introduction

The collection rate of the charge carriers in solar cell depends on the diffusion length of electrons and holes. In general, minority carrier diffusion length (i.e. less mobile) are hardly measured in comparison with the more mobile type charge carriers (i.e. electrons). Though, most of the methods suggested for the determination of the minority carrier diffusion length are suitable for crystalline silicon material where length is large (typically > 10 μm) [1, 2]. A few methods were suggested to measure the diffusion related quantity in photoconductive semiconductor thin film, such as

*Corresponding author. Tel.: +91 11 45608650; Fax: +91 11 45609310; E-mail: skumar@nplindia.org

hydrogenated amorphous silicon (a-Si:H), nano (nc-Si:H) and micro-crystalline silicon (μc-Si:H), polymorphous silicon, where diffusion length is small.

Photoconductive semiconductor thin film deposited on insulating substrate has minority carriers' diffusion length between tenths of nm to few micro-meters (typically less than 500 nm) and has dark resistivity of l06- l09 ⍰ cm. nc-Si:H/ μc-Si:H is a mixed phase film in which crystallites structure are embedded in the amorphous matrix. Since, the diffusion length of the carriers is very short in silicon thin film so the transport mechanism in a solar cell is considered to be drift assisted where the collection of the carriers depends on the strength of the built-in-electric field (Eb) and mobility of the minority carrier [3, 4]. In P-I-N configuration-based silicon thin film solar cell, absorption of photon; creation of an electron-hole pair and transport of charge carriers towards the respective electrodes occur in the intrinsic layer of the solar cell. If the built-in-electric field is strong in P-I-N junction which usually occurs when intrinsic layer typically less than 200 nm, in this case the charge transport towards the respective electrode (i.e. holes from i-layer drift towards p-side and electron from i-layer drifts towards n-side) is drift assisted and hence carrier loss depends on the strength of built-in-electric field. Though, if the built-in-electric field is weak which occurs when intrinsic layer thickness is more than 200 nm, in this the carrier transport is diffusion type and the carrier loss depends on the diffusion length of charge carriers [5]. The former case where intrinsic layer thickness is less than 200 nm could be considered in the short circuit region of P-I-N configuration whereas later case in which the intrinsic layer thickness is more considered in an open-circuit region. Thus, if the diffusion length is much smaller than the intrinsic layer thickness, the fill factor of the P-I-N configuration based solar cell will be reduced due to carrier recombination near the open-circuit region and hence the efficiency of solar cell also decreases. A measurements of the diffusion related quantity which further depends on mobility of the minority carrier and the duration of its contribution to current may be expected to be of importance in determining efficiency of P-I-N thin film solar cell.

Presently, the solar energy production based on silicon thin film technology has widen of the scope for highly efficient and stable solar panels recently with the concept of multi-junctions and Heterojunction with Intrinsic Thin layer (HIT) solar cells [6-8]. In silicon thin films, the majority charge carrier (i.e. electrons) mobility lifetime could be measured from photoconductivity (σ_{ph}) as [9]

$$\sigma_{ph} = eG\mu\tau \quad (1)$$

where G is the carrier generation rate, τ is the life time of electron, μ is the mobility of electron. For a thin film of thickness d, the generation rate of photo-carriers, G, can be expressed as [10]

$$G = \eta I_o(1-R)[1-e^{-\alpha d}]/d \quad (2)$$

where η is the quantum efficiency of the generation of photo-carriers, Io is the number of incident photons per unit area (photon flux), R is reflectivity and α is the absorption coefficient. However, the experimental determination of the minority carrier diffusion length and mobility lifetime product is more complicated. The steady state photo-carrier grating (SSPG) technique has been introduced by Ritter, Zeldov and Weiser; considered as a simple and convenient way to measure the minority carrier diffusion length in photoconductive semiconductor film [11-13].

In the SSPG technique two laser beams L1 and L2 of λ wavelength incident on the same area of a semiconductor by making an angle θ between them where they undergo refraction and creates an interference pattern with a grating period Λ, given by the equation [14]

$$\Lambda = \frac{\lambda}{2\sin\frac{\theta}{2}} \qquad (3)$$

The arrangement of two monochromatic and coherent interfering light beams was shown in figure 1 (a). The interference inside the semiconductor results as a high and low intensity fringes produces a photo-carrier grating (G (x,y,z)) where the carrier concentration varies with the intensity of the fringes as [15]

$$G\ (x, y, z) \approx G(x) = G_1 + G_2 + 2\gamma_o\sqrt{(G_1G_2)}\cos\frac{2\pi x}{\Lambda} \qquad (4)$$

where G1 and G2 are the photo-generation rates resulting from beams L1 and L2, respectively and γo is the contrast of the interference pattern, the ideal value being γo = 1. Photo-carrier grating is formed due to the difference in the diffusion length of the electrons and holes [16]. Since the diffusion length of electrons is higher than holes, hence electrons are distributed more evenly between the region of high and low intensity fringes than the holes. Hence, in the first half of the grating period there are more holes than electrons while in the second half there is a larger deficiency of holes than of electrons. The schematic representation of this photo-carrier grating was shown in figure 1 (b). A well-defined photo-carrier grating is created in the semiconductor if the grating period (Λ) is much larger than the carrier diffusion length (L) else uniform illumination pattern will result [13]. The photo-carrier grating amplitude could be measured either through measuring the photocurrent or through photo-conductivity measurement. Since, the photo-carrier grating causes a change in the photo-conductivity of the thin film due to space charge creation which is also linked to the trapping of minority carrier, as [12]

$$\sigma_1 = B_oG_1^{\gamma} \qquad (5)$$

where Bo is a constant and γ is the photo-conductivity exponent. The grating minima have a lower conductivity than the average conductivity, the photocurrent in this direction is lower than in the case when no grating is present. Thus, from the magnitude of the photocurrent measured as a function of the grating period, the ambipolar diffusion length can be estimated [11]. The area of illumination is chosen in between two parallel electrodes deposited on top of the thin film semiconductor, the gap in between the coplanar electrodes being of the order of a millimetre.

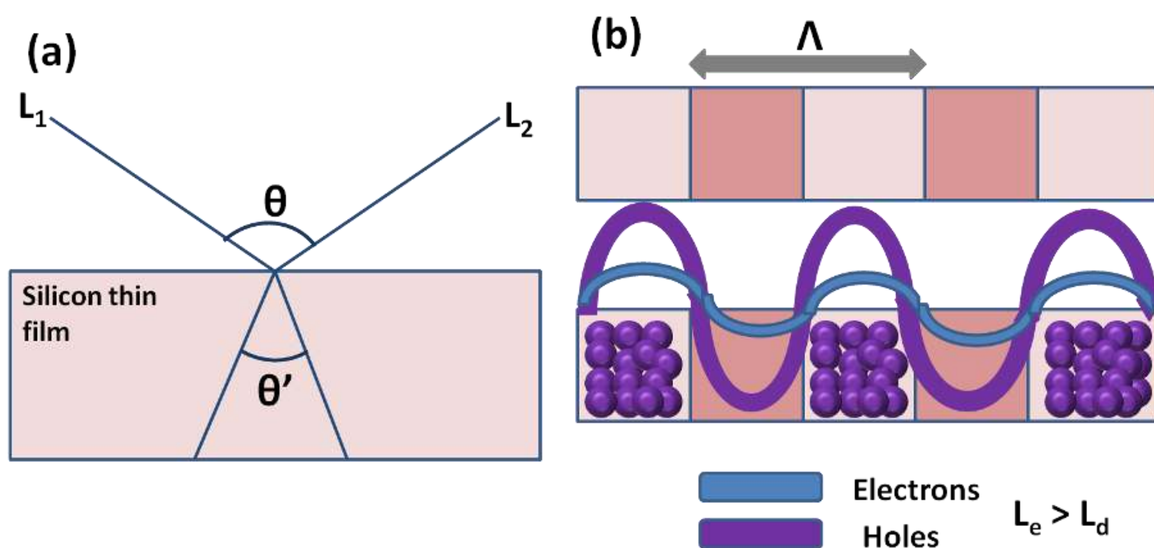

Figure 1 (a) Representation of two coherent light incidents on silicon thin film and undergo refraction and form photo-carrier grating in the sample **(b)** An illustration of the distribution of the holes and electrons in the photo-carrier grating configuration.

Figure 1 (a) Representation of two coherent light incidents on silicon thin film and undergo refraction and form photo-carrier grating in the sample (b) An illustration of the distribution of the holes and electrons in the photo-carrier grating configuration.

Among the various precautions one must take to avoid inaccurate results by the large amplitude attenuated intensity of one of the laser beams with respect to the other laser beam in order to get interference fringes. To the best of our knowledge, this concept has not been mentioned until now and if not done carefully it can lead to large errors in the measured Ld. In addition to that the variation of ambipolar diffusion length with respect to different order photo-gain a-Si:H thin film and different crystalline volume fraction of nc-Si:H/μc-Si:H film was also represented in the present study

2. Materials and methods

An experimental setup for measuring the ambipolar diffusion length by SSPG technique at room temperature was shown in figure 2. The SSPG measurements were carried out using a He-Ne laser of the wavelength of 632.8 nm with a photon flux density of 10^{17} cm^{-2} s^{-1}. A beam splitter divided the laser beam in two beams by making an angle θ between them. The two beams superimposed on the thin film by means of two mirrors (M_1 and M_2) and three polarisers (P_1, P_2 and P_3). In order to obtain high-quality interference fringes the optical path length of both beams from the beam splitter to thin film must be lower than the coherent length of the light. The experimental conditions for the measurement of L_d are such that one of the laser beams is called main beam (L_1) and another beam is used as a probe beam (L_2). The intensity of the probe beam is attenuated with a neutral density filter (ND) and chopped at low frequency. The intensity of the main beam is not attenuated but the polarization of the light can be modified by means of a polariser. Two polarisers P_1 and P_2 are introduced in the path of strong beam where the polariser P_3 is placed in the path of probe beam. P_2 is kept at ± 45° with respect to the plane of polarisation of P_1. Furthermore, the two position of P_2 are such that its plane of polarisation is either perpendicular or parallel to that of P_3. Thus, P_2 act as a half wave plate as the rotation of P2 by 45° changes the polarisation of the laser beam by 90°. Finally, the photocurrents ($I_{\perp}$; $I_{\parallel}$) are measured with a lock-in amplifier synchronized with the chopper across a series resistance (5 MΩ) in two conditions, namely at the polarizations of the two light beams are crossed or the polarisation of the light beam are same.

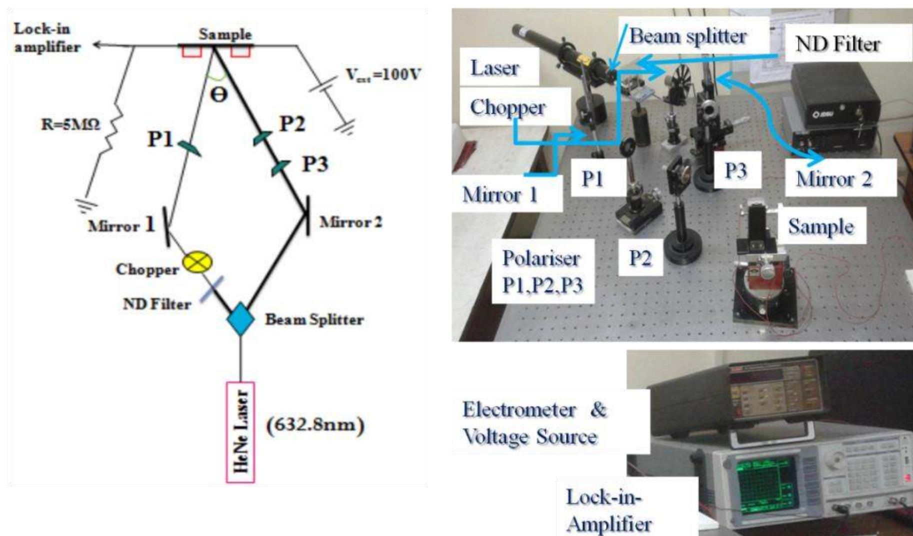

Figure 2 Layout diagram of the SSPG used in present experimentation.

In the former case photo-current flowing into the sample due to the addition of the probe beam onto the main beam whereas in the later case one can measure the photo-current due to the creation of interference pattern between the main and probe beams. RZW analysis related ratio of these photocurrent in the photo-carrier grating condition ($I_{\parallel}$: parallel polarization) to that in the no grating condition ($I_{\perp}$: perpendicular polarization), β parameter with the ambipolar diffusion length L_d according to [17]

$$\beta = \frac{I_{\parallel}}{I_{\perp}} = 1 - \frac{2Z}{\left[1+\left(\frac{2\pi L_d}{\Lambda}\right)^2\right]^2} \quad (6)$$

where, Z is a fit parameter which contains information on the grating quality. The typical value of Z lies between 0.5 and 1. The chopping frequency while measuring photo-current is set to low enough i.e. on 17 Hz. At such a low frequency, the phase lag is less than 1°, indicating that the steady state approximation is applicable. The sample holder is moved to various positions to change the grating period (Λ) which is linked to the angle in between the two beams and hence accordingly the mirrors and the optics are aligned approximately to produce interference fringes at the thin film. A small bias voltage is also applied on the electrodes of the thin film semiconductor; the magnitude of voltage was chosen after analysis that β did not depend on it which ensuring that the carrier distribution is governed by diffusion transport not by drift transport. The electric field applied between the contacts was 100 V/cm.

From a measured set of β values at a number of Λ positions, a fit can be made with the two fit parameters L_d and Z. The above equation can be changed in the linear equation form (y=mx+c) as

$$(1-\beta)^{-\frac{1}{2}} = ((2Z)^{-\frac{1}{2}} {L_d}^2)\left(\frac{2\pi}{\Lambda}\right)^2 + (2Z)^{-\frac{1}{2}} \quad (7)$$

where measured β values plotted as ordinate values and L_d and Z evaluate from linear fits. The L_d is related to the product of mobility (μ) and the recombination time (τ) of the minority carriers as [14]

$$L_d = \sqrt{\frac{2e(\mu\tau)_{min}}{kT}} \quad (8)$$

where, k is the Boltzmann constant and kT is the thermal energy.

An SSPG measurement has been carried out on the intrinsic layer of a-Si:H/nc-Si:H/μc-Si:H silicon thin film. The silicon thin films were deposited on Corning 7059 glass using a capacitively coupled PECVD system having an inter-electrode gap of 12 mm and area 113 cm^2. 5 % Silane (SiH_4) diluted in H_2 was used as the precursor gas. The other deposition conditions such as Silane flow rate, substrate temperature, chamber pressure and applied power were listed in Table 1 with the reference of the previous published paper of our group where the structural, optical and electrical properties were presented with the growth conditions [18-23].

Raman spectra were recorded in the back-scattering mode at room temperature using 514.5 nm excitation wavelength obtained from Argon laser in Raman microprobe. Under the typical conditions the coplanar Aluminium (Al) contact geometry having a gap of 0.78 mm was deposited on silicon thin films using thermal evaporation technique. In order to estimate photo-gain {($\psi = \sigma_{ph} / \sigma_d$) (dark conductivity ($\sigma_d$), photoconductivity ($\sigma_{ph}$)} dark conductivity and photoconductivity of the deposited films was measured using a Keithley electrometer with coplanar Al contact geometry. Photoconductivity measurement was made under white light illumination of intensity ~ 100 mW/cm^2.

Table 1: Process conditions of a-Si:H/μc-Si:H/nc-Si:H deposited film

Sample no.	Applied power density (mW/cm²)	Chamber Pressure (Torr)	SiH_4 flow rate (sccm)	Substrate Temperature (°C)	Phase of thin film	Reference of our recent publication
S1	35	0.53	47	270	a-Si:H	[18]
S2	88	0.53	47	270	a-Si:H	[19]
S3	35	0.33	47	270	a-Si:H	[18]
S4	88	0.13	47	270	a-Si:H	[19]
S5	88	0.43	SiH_4+Ar	270	μc-Si:H	[20]
S6	265	0.23	47	270	nc-Si:H	[21]
S7	133	0.23	47	270	nc-Si:H	[22]
S8	177	0.53	47	270	nc-Si:H	[23]
S9	177	0.23	47	270	nc-Si:H	[22]

3. Results and discussion

3.1 Intensity variation

In order to observe the effect on ambipolar diffusion length from the variable range of attenuated intensity probe beam; the intensity of the probe beam is attenuated with respect to fixed intensity main beam by a factor of 20 % to 99 % with the use of Neutral Density filter (ND). The fraction of the light attenuated through the filter can be calculated as

$$10^{-d} = \frac{I}{I_o} \qquad (9)$$

where I_o is the incident intensity, I is the attenuated laser intensity and d is Optical Density value of filter (this is a measure of how much light is blocked by a filter). In this experimentation optical density value of filter was varying from 0.1 to 1.0.

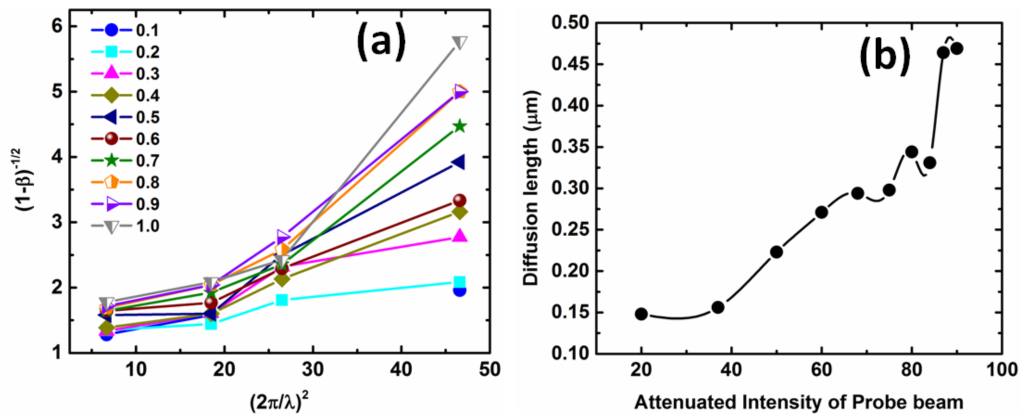

Figure 3 (a) Linear fit of Balberg plot at different optical density value of ND filter **(b)** Variation of ambipolar diffusion length with respect to attenuated probe beam intensity**.**

For the estimation of L_d, the Balberg plot of a-Si:H deposited thin film at various optical density value of ND filter was shown in figure 3 (a). The estimated value of L_d was found to vary from 0.148 µm to 0.469 µm as the attenuation of the intensity of probe beam increases from 20 % to 99 %. The variation of the same was plotted in figure 3 (b). From these results one can see that till 38 % attenuated probe beam light, the value of ambipolar diffusion length is nearly same but beyond that there is a significant increase in L_d was observed. Shorten photo-carrier grating due to very weak intensity probe beam might be the possible reason for this trend. This causes β to have a larger value and hence the inferred diffusion length will be larger than is actually the case.

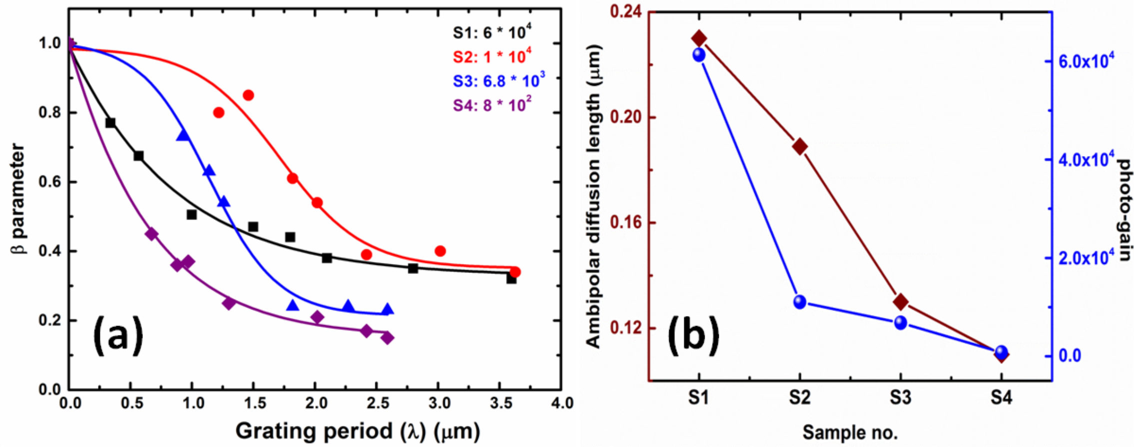

Figure 4 (a) Balberg plot of different photo-gain a-Si:H thin film **(b)** Variation of ambipolar diffusion length with respect to photo-gain of a-Si:H thin film.

3.2 With Photo-gain variation

Photo-gain ($\psi = \sigma_{ph}/\sigma_d$) of the deposited a-Si:H films can be estimated by dark conductivity (σ_d) and photoconductivity (σ_{ph}). σ_{ph} in a-Si:H depends on the absorption of light, generation of electron-hole pair and at last collection of charge carriers which can escape recombination before reaching the electrodes. The values of σ_d and σ_{ph} were illustrated in Table 2 which leads to increase the photo-gain from 8 x 10^2 to 6.0 x 10^4 for deposited films. In order to illustrate the effect of ψ on ambipolar diffusion length, different order of ψ a-Si:H thin films was chosen. figure 4 (a) shows the Balberg plot of deposited a-Si:H thin film at various photo-gain. The variation of L_d w.r.t photo-gain was depicted in figure 4 (b) and the value of $(\mu\tau)_{min}$ was listed in Table 2. From these results one can see higher the order of ψ, higher the value of L_d, hence there was a correlation observed for photo-gain with ambipolar diffusion length. The variation of L_d could be associated with low recombination of photo generated carriers at higher value of ψ.

Table 2: Estimated value of dark conductivity (σ_d), photoconductivity (σ_{ph}) and minority carrier mobility lifetime product ($(\mu\tau)_{min}$) of deposited a-Si:H thin films.

Sample No.	σ_d (ohm^{-1}cm^{-1})	σ_{ph} (ohm^{-1}cm^{-1})	$(\mu\tau)_{min}$ (cm^{2}V^{-1})
S1	1.33 x 10^{-10}	8.16 x 10^{-6}	0.54 x 10^{-8}
S2	1.63 x 10^{-9}	1.81 x 10^{-5}	0.47 x 10^{-8}
S3	6.39 x 10^{-9}	4.36 x 10^{-5}	0.32 x 10^{-8}
S4	1.24 x 10^{-9}	9.96 x 10^{-7}	0.16 x 10^{-8}

3.3 With Crystalline content

The Raman spectra of μc-Si:H/nc-Si:H films recorded in the range 350 cm^{-1} to 650 cm^{-1} was shown in figure 5 (a). The Raman peak at~ 480 cm^{-1} corresponds to the Transverse Optic (TO) mode of amorphous Si-Si vibrations while TO peak shifts towards the higher wave number i.e. towards 520 cm^{-1} may be associated with the presence of small crystallites [24]. The Raman spectra of S5 thin film corresponds to a μc-Si:H structure whereas S6 – S9 deposited film corresponds to a nc-Si:H structure. The structural, optical and electrical properties of S5-S9 deposited films were reported in our recent publication [20-23]. To estimate crystalline volume fraction (X_c) of these deposited films one may de-convolute the spectra into three Lorentzian parts was shown in figure 5 (b) and defined as

$$Xc = \frac{I_c}{I_c + I_g + I_a} \tag{10}$$

where I_c, I_g and I_a are the integrated area of crystalline (peak position = 520 cm^{-1}), grain boundaries (500 cm^{-1}) and amorphous (480 cm^{-1}) dominated region [25]. Xc of deposited thin films were listed in Table 3.

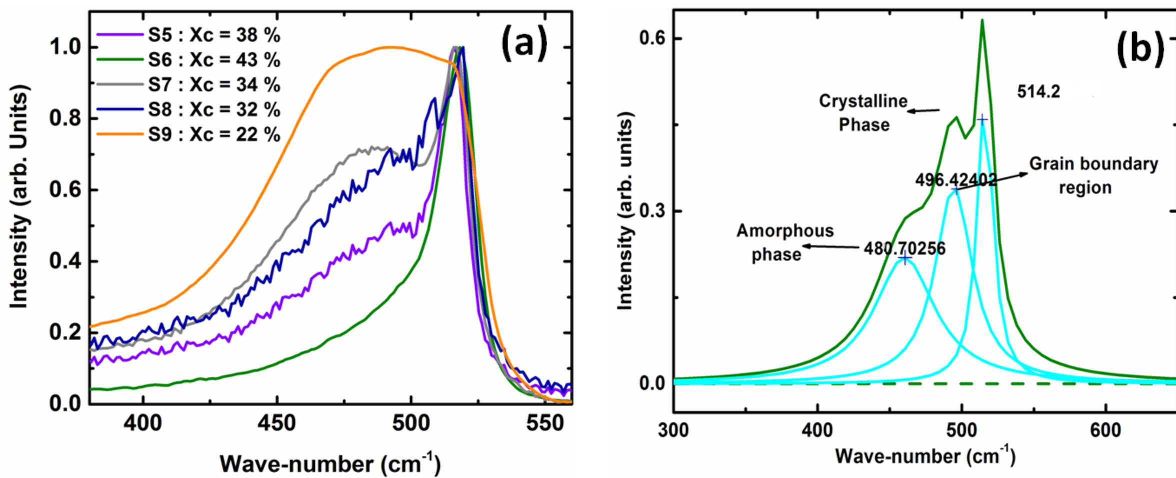

Figure 5 (a) Raman spectra of S5-S9 nc-Si:H/μc-Si:H thin film **(b)** De-convolution of Raman Spectra

Since nc-Si:H/μc-Si:H film is a mixed phase structure as it consists of crystallites, grain boundary and amorphous content which shows much more complicated transport mechanism than single phase a-Si:H. The electrical properties of nc-Si:H/μc-Si:H depends implicitly on the crystalline volume fraction and transport pathway of the carriers. Rezek et al and Kocka et al was proposed that, if the crystalline fraction (X_c) of the deposited film is high enough in that case percolation might take place [26, 27] and charge carriers might mainly transport through interconnected crystallites which are embedded in percolation path and have to pass the grain boundaries to reach the contacts; and if the X_c is low, then percolation pathway disappears due to the significant potential barriers between the isolated crystallites in the form of grain boundaries.

Table 3: Crystalline volume fraction (Xc), Crystallite size (D), dark conductivity (σ_d), photoconductivity (σ_{ph}) and minority carrier mobility lifetime product ($(\mu\tau)_{min}$) of deposited nc-Si:H/μc-Si:H thin films.

Sample No. and phase of the film	X_c (%)	σ_d ($ohm^{-1}cm^{-1}$)	σ_{ph} ($ohm^{-1}cm^{-1}$)	$(\mu\tau)_{min}$ (cm^2V^{-1})
S5 (μc-Si:H)	38	117 x 10^{-9}	4.9 x 10^{-6}	0.62 x 10^{-8}
S6 (nc-Si:H)	43	7307 x 10^{-9}	48 x 10^{-6}	0.47 x 10^{-8}
S7 (nc-Si:H)	34	4200 x 10^{-9}	37 x 10^{-6}	0.34 x 10^{-8}
S8 (nc-Si:H)	32	203.7 x 10^{-9}	29.58 x 10^{-6}	0.35 x 10^{-8}
S9 (nc-Si:H)	22	14.7 x 10^{-9}	0.205 x 10^{-6}	0.11 x 10^{-8}

The estimated value of the dark-conductivity and photo-conductivity of S5 – S9 deposited films was depicted in Table 3. From here, it can be seen that that the σ_d of S5-S8 nc-Si:H/μc-Si:H deposited films was higher than that of S1- S4 a-Si:H films. In order to estimate the minority carrier transport properties in S6-S9 deposited films the Balberg plot was shown in figure 6 (a) shows and the estimated value of L_d w.r.t X_c was shown in figure 6 (b). These results depict that higher the value of crystalline volume fraction, higher its ambipolar diffusion length. This indicates that the X_c of these films exceeds the percolation threshold which was observes to a cause an increase of the σ_d and L_d as a result of this carriers does not travelled the prolonged distance in amorphous region as they pass through in crystallite pathway. On the other hand, for S9 deposited nc-Si:H film low σ_d and low L_d was observed. Since in this case low value of X_c was estimated in comparison with other nc-Si:H/μc-Si:H films. Hence due to lower value of X_c, an isolated crystallite will exist apart from the percolation paths by thick grain boundaries and hence carriers generated in these isolated crystallites will experience the high series of resistance, thus their contribution to the secondary current is lower than the contribution of carriers generated in amorphous fraction, as a result low L_d and σ_d was observed.

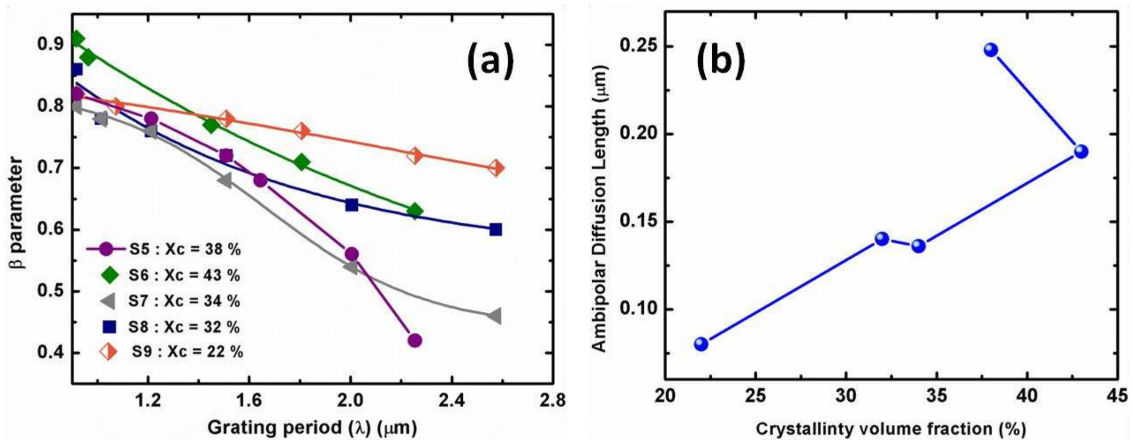

Figure 6 (a) Balberg plot of different crystalline volume fraction μc-Si:H/nc-Si:H thin film **(b)** Variation of ambipolar diffusion length with respect to crystalline volume fraction μc-Si:H/nc-Si:H thin film

4. Conclusions

Here, we have considered the effect of the larger attenuated intensity of the probe laser beam (L_2) with respect to main laser beam (L_1) for the interference fringes, and find that till 38 % attenuated

probe beam light, the value of ambipolar diffusion length is same but beyond that, which is from 50 % to 90 % measured value of L_d will be larger than the appropriate value. The appropriate e L_d of our a-Si:H sample is 0.148 μm which has been observed till 38 % attenuated probe beam light. However, the measured L_d increases as the attenuation in the probe laser light increases which occurs due to the shorten photo-carrier grating. Furthermore, in the present study we have also seen that higher the order of photo-gain in a-Si:H deposited films and higher the value of crystalline volume fraction in nc-Si:H/μc-Si:H films, higher its ambipolar diffusion length. These findings will help to understand the transport properties of silicon thin films and thus designing efficient, high ambipolar diffusion length intrinsic layer for p-i-n configuration based thin film silicon solar cell applications.

Acknowledgements

The authors are grateful to Director, CSIR National Physical Laboratory, New Delhi (India) for his kind support. We are also thankful to Dr. Bhanu Pratap Singh from NPL, New Delhi for extending Raman Spectroscopy. We are also thankful to Ms Kalpana Lodhi and Ms Arti Rawat for providing the help during experimentation setup. We also acknowledge CSIR-India for TAPSUN program and MNRE, Govt. of India for the research grant (sanction 31/29/2010-11/PVSE).

References

1. Borrego, J. M., Gutmann, R. J., Jensen, N., & Paz, O.: Non-destructive lifetime measurement in silicon wafers by microwave reflection. Solid-state electronics 30, 195-203 (1987).
2. Sarîtas, M., & McKell, H. D.: Comparison of minority-carrier diffusion length measurements in silicon by the photoconductive decay and surface photovoltage methods. Journal of applied physics 63, 4561-4567 (1988).
3. Moore, A. R.: Diffusion Length in Undoped a-Si: H. Semiconductors and Semimetals, 21, 239-256 (1984).
4. Faughnan, B., Moore, A., & Crandall, R.: Relationship between collection length and diffusion length in amorphous silicon. Applied Physics Letters, 44, 613-615 (1984).
5. Poortmans, Jef, and Vladimir Arkhipov, eds.: Thin film solar cells: fabrication, characterization and applications. Vol. 18. John Wiley & Sons, (2006).
6. Kim, S., Chung, J. W., Lee, H., Park, J., Heo, Y., & Lee, H. M.: Remarkable progress in thin-film silicon solar cells using high-efficiency triple-junction technology. Solar Energy Materials and Solar Cells, 119, 26-35(2013).
7. Matsui, T., Sai, H., Saito, K., & Kondo, M.: High-efficiency thin-film silicon solar cells with improved light-soaking stability. Progress in Photovoltaics: Research and Applications, 21, 1363-1369 (2013).
8. Taguchi, M., Yano, A., Tohoda, S., Matsuyama, K., Nakamura, Y., Nishiwaki, T., ... & Maruyama, E.: 24.7% record efficiency HIT solar cell on thin silicon wafer. IEEE Journal of Photovoltaics, 4, 96-99(2014).
9. Bronner, W., Kleider, J. P., Brüggemann, R., & Mehring, M: Defects and transport properties of electron-irradiated microcrystalline silicon with successive annealing. Thin Solid Films, 427, 51-55 (2003).
10. Chaudhuri, P., Ray, S., & Barua, A. K.: The effect of mixing hydrogen with silane on the electronic and optical properties of hydrogenated amorphous silicon thin films. Thin Solid Films, 113, 261-270 (1984).

11. Ritter, D., Zeldov, E., & Weiser, K.: Steady-state photocarrier grating technique for diffusion length measurement in photoconductive insulators. Applied Physics Letters , 49, 791-793 (1986).
12. Ritter, D., Weiser, K., & Zeldov, E.: Steady-state photocarrier grating technique for diffusion-length measurement in semiconductors: Theory and experimental results for amorphous silicon and semi-insulating GaAs. Journal of Applied Physics, 62, 4563-4570 (1987).
13. Ritter, D., Zeldov, E., & Weiser, K.: Diffusion length measurements in a-Si: H using the steady state Photocarrier grating technique. Journal of Non-Crystalline Solids, 97, 571-574 (1987).
14. Brüggemann, R.: Steady-state photocarrier grating technique for the minority-carrier characterisation of thin-film semiconductors. In Journal of Physics: Conference Series, vol. 253, p. 012081. IOP Publishing, (2010).
15. Yadav, D., & Agarwal, S. C.: Measurement of the diffusion length of minority carriers using a steady-state photocarrier grating. Solid State Communications, 150, 321-324 (2010).
16. Balberg, I.: Theory of the small photocarrier grating under the application of an electric field." Physical Review B, 44, 1628-1645 (1991).
17. Longeaud, C.: An automated steady state photocarrier grating experiment." Review of Scientific Instruments, 84, 055101(2013).
18. Sharma, M., Juneja, S., Sudhakar, S., Chaudhary, D., & Kumar, S.: Optimization of a-Si: H absorber layer grown under a low pressure regime by plasma-enhanced chemical vapor deposition: Revisiting the significance of the p/i interface for solar cells. Materials Science in Semiconductor Processing, 43, 41-46 (2016).
19. Chaudhary, D., Sharma, M., Sudhakar, S., & Kumar, S.: Effect of Pressure on Bonding Environment and Carrier Transport of a-Si: H Thin Films Deposited Using 27.12 MHz Assisted PECVD Process. Silicon, 1-7 (2016).
20. Chaudhary, D., Sharma, M., Sudhakar, S., & Kumar, S.: Investigation of powder dynamics in silane-argon discharge using impedance analyser. Physics of Plasmas, 23, 123704 (2016).
21. Sharma, M., Chaudhary, D., Sudhakar, S., Singh, P., Srivatsa, K. M. K., & Kumar, S.: Spectroscopic identification of ultranano-crystalline phases within amorphous/nano-crystalline silicon. Advanced Materials Letters, 8, 163-169 (2017).
22. Chaudhary, D., Sharma, M., Sudhakar, S., & Kumar, S.: A Novel Approach for Investigating a Phase Transition from a-Si: H to nc-Si: H. Plasma Chemistry and Plasma Processing, 37, 189-205 (2017).
23. M. Sharma, D. Chaudhary, S. Sudhakar, P. Singh, K. M. K. Srivatsa, and S. Kumar.: Investigation of structural aspect in terms of atypical phases within material deposited for a-Si: H solar cell fabrication. Advanced Materials Proceedings, 1, 32-37 (2017).
24. Smit, C., Van Swaaij, R. A. C. M. M., Donker, H., Petit, A. M. H. N., Kessels, W. M. M., & Van de Sanden, M. C. M.: Determining the material structure of microcrystalline silicon from Raman spectra. Journal of applied physics, 94, 3582-3588 (2003).
25. Min, C., Weijia, Z., Tianmin, W., Fei, J., Guohua, L., & Kun, D.: Nanocrystalline silicon films with high conductivity and the application for PIN solar cells. Vacuum, 81, 126-128 (2006).
26. Kočka, J., Fejfar, A., Mates, T., Fojtík, P., Dohnalová, K., Luterová, K., ... & Ito, M.: The physics and technological aspects of the transition from amorphous to microcrystalline and polycrystalline silicon. physica status solidi (c), 1, 1097-1114 (2004).
27. B Rezek, B., Stuchlık, J., Fejfar, A., & Kočka, J.: Local characterization of electronic transport in microcrystalline silicon thin films with submicron resolution. Applied physics letters, 74, 1475-1477 (1999).